Magnetic properties resulting from core-shell interactions in nanosized $Ni_{0.25}Co_{0.25}Zn_{0.5}Fe_2O_4$

N. Lakshmi, Hina Bhargava, O. P. Suwalka, and K. Venugopalan
Department of Physics, Mohanlal Sukhadia University, Udaipur, 313 001 Rajasthan, India

Varkey Sebastian
Department of Physics, Nirmalagiri College, Kuthuparamba, Kerala 670701, India

V. R. Reddy and Ajay Gupta
UGC-DAE Consortium for Scientific Research, Khandwa Road, Indore 452001, India

(Received 9 June 2009; revised manuscript received 3 November 2009; published 25 November 2009)

Nanosized particles of $Ni_{0.25}Co_{0.25}Zn_{0.5}Fe_2O_4$ have been synthesized by chemical coprecipitation method. Exchange-bias phenomenon arising from the core-shell interaction has been investigated using a combination of in-field, low-temperature Mössbauer spectroscopy and dc magnetization. To understand the clear mechanism of interaction and exchange bias, isothermal remanence magnetization-dc demagnetization and *M-H* loops at different cooling field have been taken. The observed variation in coercivity H_C and exchange-bias field H_E confirms that only core is affected by the cooling field. The slope of the Henkel plot is 1.82, indicating the noninteracting nature of the particles. In-field Mössbauer spectroscopy clearly establishes the core and shell contributions and also confirms that 70% of spins are in the shell. The barrier energy has been estimated to be 17×10^{-14} ergs which accounts for the fact that the shell is not affected by application of as large a field as 5 T.

DOI: 10.1103/PhysRevB.80.174425 PACS number(s): 75.75.+a

I. INTRODUCTION

Ultrafine particles containing iron exhibit a wide range of interesting magnetic properties, depending on the presence of different magnetic phases and their mutual interactions. A thorough understanding of the mutual interaction between the core-shell phases and their effect on the overall magnetic properties is required for optimum utilization of these systems in areas such as biomedicine,[1] magnetic separation of biological particles,[2] ferrofluids,[3] and novel techniques in high-density recording such as patterned magnetic recording media.[4] In the nanoregime, contribution to the overall magnetic behavior from surface spins is considerable—increasing with decrease in the particle size to the extent of more than 50% of the spins being at the surface for sizes of 4 nm and less. Isolated noninteracting magnetic particles can be approximated to single large isolated spins described by superparamagetism which only hold good in very dilute systems. However, in real systems, the interparticle interactions become significant, leading to enhanced coercivity and exchange anisotropy,[5] and as a result, it is possible to have a variety of magnetic configurations in such systems due to competing energy terms under different conditions of applied fields and temperature.

Labarta *et al.*[6] have pointed out that spin canting of the surface layer in nanosized ferrimagnetic materials which results in exchange interactions between the core and shell have not been found in metallic ferromagnetic particles. An equivalent mechanism in the case of ball-milled nanocrystalline Fe is the spin-glasslike freezing at grain boundaries.[7] This indicates that the noncollinear arrangement of particle spins leading to spin canting originates from magnetic frustration of antiferromagnetically competing sublattices and mostly occurs at the surface. Nanosized spinel ferrites are thus ideal candidates for development of systems which are based on the core-shell exchange-bias property.

Spinel ferrites have at least two nonequivalent sublattices—generally designated as the tetrahedral *A* and octahedral *B* sites in which the magnetic ions are accommodated leading to a variety of magnetic properties depending on the site occupancy. In nanosized spinel ferrites, although on an average the cation distribution between available sites may be the same throughout the particle, two distinct magnetic phases exist due to spins on the surface and from those in the core. Measurements in high external fields give information about the sense of sublattice magnetization and also enable the separation of core and shell contributions. To observe the individual contributions, a combination of methods such as dc magnetization studies which monitor the overall contributions and microscopic observations which are sensitive to much shorter-range effects are necessary. In-field Mössbauer spectroscopy has been found to be a powerful tool for this purpose.[8] A recent study on 15-nm-sized Ni ferrite has established that external fields above 3 T reduce the number of disordered spins and so are capable of expansion of the core, thus reducing the influence of the spin-disordered surface.[9]

In this paper, we have used a combination of low-temperature dc magnetization and low-temperature Mössbauer measurements to confirm the nature of interactions and also separate the core and shell contributions to the magnetization in very fine (~ 3 nm) particles of Ni-substituted cobalt zinc ferrite. Mössbauer measurements have been made at 10 K with no applied field and since Mössbauer measurements with large applied fields give valuable information about magnetic ordering, spectra have also been recorded at

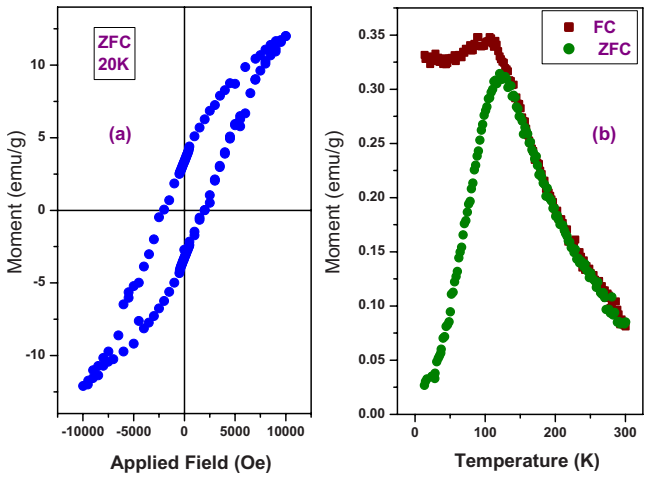

FIG. 1. (Color online) (a) ZFC *M-H* curve at 20 K and (b) FC, ZFC measurements at applied field of 50 Oe.

5 K with applied field. Magnetic field has been applied parallel and perpendicular to γ-ray direction after zero-field cooling (ZFC) and in perpendicular direction after field cooling (FC). Unlike in the case of Ni-ferrite nanoparticles,[9] these experiments show that the spin arrangement at the surface is unaffected even on application of 5 T field.

II. EXPERIMENT

Nanosized particles of $Ni_{0.25}Co_{0.25}Zn_{0.5}Fe_2O_4$ were prepared using the chemical coprecipitation method described elsewhere.[10] Formation of single-phased fine particles of average size 3 nm and lattice parameter 8.56 ± 0.015 Å was confirmed by x-ray diffraction. The average size was calculated using Scherrer formula and was also independently confirmed using transmission electron microscopy.[10] dc magnetization studies were done on a Lake Shore 7300 vibrating sample magnetometer coupled to a closed cycle refrigerator. ZFC and FC curves were recorded at a small applied dc field of 50 Oe. *M-H* curves reported in this study were recorded for a range of ± 1 T at room temperature (RT) and 20 K. Mössbauer spectra in the transmission mode were recorded at RT and 5 K both with and without applied field of 5 T for perpendicular and parallel configurations using a JANIS SuperOptiMag system. Velocity calibration was done by recording Mössbauer spectra for Fe foils under conditions identical to those of samples.

III. RESULTS

A. dc magnetization studies

M-H loop recorded at RT for this sample shows it to be superparamagnetic as expected for particles of 3 nm size as in the present sample. The blocking temperature T_B has been determined to be 123 ± 1 K from the ZFC curve [Fig. 1(b)] recorded at a field of 50 Oe. From the value of T_B and particle size V, the anisotropy energy K, the energy barrier ΔE for rotation on applying a field H, and anisotropy field H_k can be estimated using the following expressions:[11,12]

$$K = \frac{25 k_B T}{V}, \tag{1}$$

$$\Delta E = KV\left(1 - \frac{H}{H_k}\right)^2, \tag{2}$$

where, k_B is the Boltzmann constant, $H_k = \frac{2K}{M_s}$ is the anisotropy field, and M_s is the saturation magnetization. Accordingly, calculating these values using Eqs. (1) and (2) K equals to 1.08×10^7 ergs/cm^3, H_k is about 22 T, and ΔE at an applied field H of 5 T, used in the in-field Mössbauer studies, is about 17×10^{-14} ergs. M_s has been estimated by extrapolating the M vs $1/H$ for $1/H$ tending to zero.

To check for the presence of exchange biasing induced by the highly disordered surface, *M-H* loops (Fig. 2) have been recorded after cooling the sample down to 20 K in the presence of different values of applied fields termed as cooling

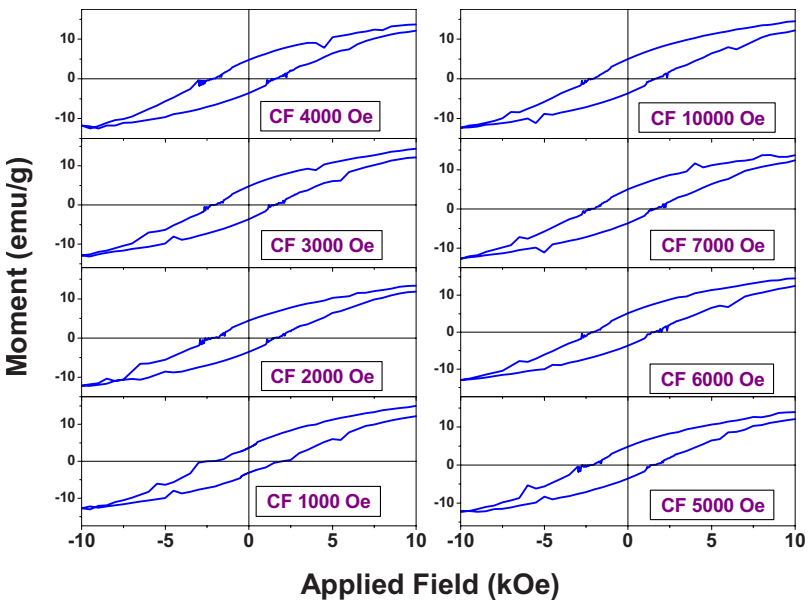

FIG. 2. (Color online) *M-H* loops at 20 K recorded for various CFs.

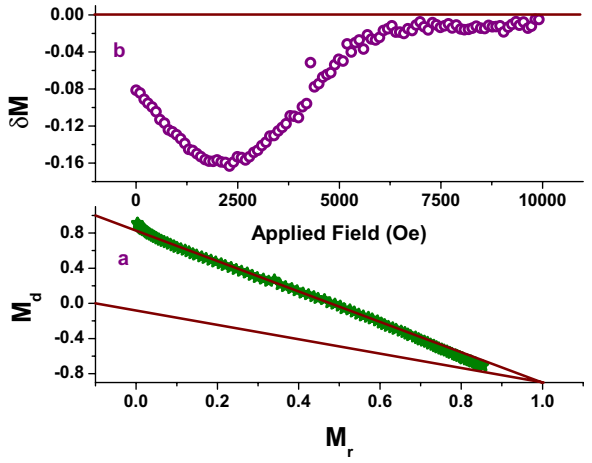

FIG. 3. (Color online) (a) Henkel plot and (b) δM plots.

field (CF). The M-H loop recorded at 20 K with zero applied field is closed and symmetric about both axes [Fig. 1(a)] while those recorded after field cooling are open due to irreversibility caused by field cooling. A systematic shift in the loop to the left is apparent on field cooling and originates from the phenomena of exchange bias[13–16] associated with the exchange anisotropy created at the interface between antiferromagnetic (AFM) and ferromagnetic (FM) phases as first observed in nanosized oxidized Co nanoparticles.[13]

Exchange bias is usually observed when a material having FM/AFM interfaces is cooled in the presence of a static magnetic field, through the Neel temperature (T_N) of the AFM phase (with Curie temperature, T_C, of the FM phase larger than T_N). After field cooling, the hysteresis loop of the FM-AFM system is shifted through a value called exchange-bias field, H_E, along the field axis generally in a direction opposite (negative) to the cooling field. The exchange-bias field is usually taken as the shift of the center of the hysteresis loop along the field axis and the coercivity as the half width of the loop. In the present system, exchange bias originates from the coupling between the ferromagnetic core and the disordered (antiferromagnetic) surface. The exchange-bias field and coercivity can be obtained from the switching field on the left (H_{SL}) and right (H_{SR}) branches of the loop using the following equation:[17]

$$H_E = \frac{-H_{SR} + H_{SL}}{2}, \tag{3}$$

$$H_C = \frac{H_{SR} - H_{SL}}{2}. \tag{4}$$

In the present study, H_{SR} and H_{SL} are those points at which the M-H loop cuts the field axis.

To further confirm the nature of magnetic interactions, the isothermal remanence magnetization (IRM) curve $M_r(H)$ and dc demagnetization (dcD) curve $M_d(H)$, both normalized to the saturation remanence, have been plotted at 20 K. From these curves a Henkel plot has been obtained [Fig. 3(a)]. In a perfectly noninteracting system of single-domain particles, the slope of the Henkel plot should be −2 and the experimental points will lie on the upper limit of this plot.[18] The types of interactions are characterized by means of δM plots [Fig. 3(b)] obtained using the following relation:

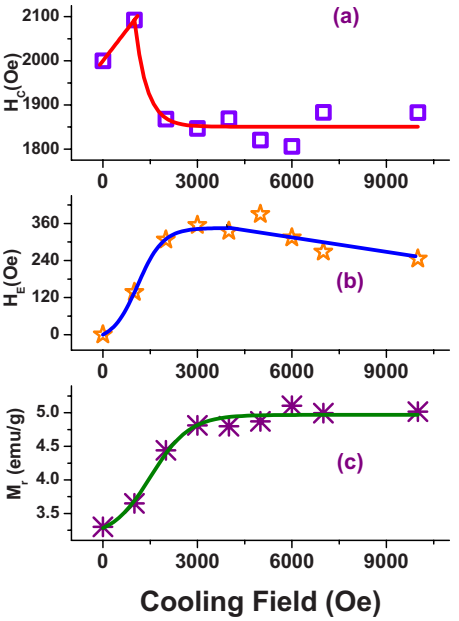

FIG. 4. (Color online) (a) Coercive field, (b) exchange-bias field, and (c) remanence as a function of the cooling field.

$$\delta M = M_d(H) - 1 + 2M_r(H). \tag{5}$$

Positive values of δM imply an exchange type of interaction which results in a magnetized state while a negative one indicates a demagnetized state attributable to presence of dipolar type of interactions.

Results of field-cooled M-H curves together with those from remanence curves taken together give a clear picture of the interaction mechanisms within each particle and that in the ensemble as a whole. Plots of variation in H_C and H_E [Figs. 4(a) and 4(b)] for different fields applied while cooling can be divided into two distinct portions—for CF from 0 to 3000 Oe and from 3000 to 10 000 Oe. The value of the coercivity H_C, at an applied field of 1000 Oe is slightly larger than its value after zero-field cooling. H_E also first increases up to 3000 Oe and then decreases. These results can be explained as follows: on cooling down to 20 K in the presence of a field of 1000 Oe, most of the core spins get aligned. The spin frustration at the surface due to disordering, broken/dangling bonds leads to spin canting so that the spins at the surface are, on an average, randomized to attain a minimum-energy configuration. This leads to a system in which the spins at the surface are effectively locked leaving the surface unaffected on application of a field. The initial decrease in H_C after field cooling on increasing the cooling field, CF, is because of magnetic softening induced in the system due to large applied fields. This is also reflected in the δM plot which is demagnetizinglike in this region. Constancy in the value of H_C beyond a CF of 2000 Oe clearly indicates that only the core is affected on application of field and that once the spins loosely bound to the surface have also aligned, further increase in the field has no effect on the system as

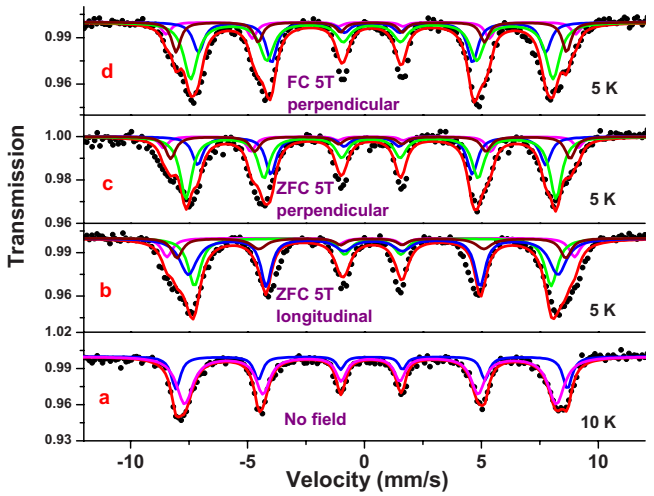

FIG. 5. (Color online) Low-temperature Mössbauer spectra with (a) no applied field, (b) field applied along the γ-ray direction, (c) field applied perpendicular to γ-ray direction after cooling down to 5 K with no applied field, and (d) field applied perpendicular to γ-ray direction after cooling down to 5 K in the presence of 5 T field.

evidenced by the very large anisotropy field H_k estimated for the present samples.

The trend in H_E [Fig. 4(b)] shows that for CF more than 3000 Oe, with increase in the CF, the magnetic coupling between the field and the surface moment also increases although the applied field is not sufficient to rotate the surface spins to align along field direction. However, increasing the cooling field also leads to an increase in the energy at the core-shell interface or in other words, the system freezes through a configuration in which the core-shell energy is not minimized. The net effect is a reduction in H_E as observed in the present study and as reported by Bianco *et al.*,[19] in their study of Fe nanoparticles embedded in Fe-oxide matrix.

Correspondingly, the value of remanence, $+M_r$, increases from its value of 12 emu/g at zero applied field to 15 emu/g which does not change with further increase in applied field [Fig. 4(c)]. Together, these results show that on application of field, the core spins get aligned while the surface is unaffected.

The totally noninteracting nature of the ensemble is evident from the Henkel plot [Fig. 3(a)] of experimentally obtained points after remanence measurements (IRM and dcD) which have a slope of −1.82 and which almost coincide with the theoretical upper limit [Fig. 3(a)]. The exchange coupling interactions between the core and shell were evaluated using δM plots [Fig. 3(b)]. There is a shallow initial negative peak which then tends to zero after about 3000 Oe. The negative peak is indicative of magnetostatic interactions which are demagnetizinglike and which favor antiferromagnetic coupling between the core and shell spins. There is no further change on application of larger fields, since, as discussed earlier, core alignment is complete and core-shell spin locking through antiferromagnetic coupling is strong.

B. Mössbauer measurement

Room-temperature Mössbauer spectra of the sample show the two doublet pattern typical of superparamagnetic particles.[10] Mössbauer spectra have been recorded at low temperatures under four different conditions—with no field applied (at 10 K), field applied after cooling to 5 K with field directions parallel ($ZFC_{parallel}$) and perpendicular ($ZFC_{perpendicular}$) to γ rays. A fourth spectrum was obtained after cooling the sample down to 5 K with an applied field of 5 T, then recording with an applied field of 5 T perpendicular to γ-ray direction ($FC_{perpendicular}$) (Fig. 5).

The spectrum obtained at zero applied field is resolved into two sextets with average hyperfine fields of 52 and 49 T corresponding to Fe at the tetrahedral A and B sites, respectively. Cation distribution at the tetrahedral A and octahedral B sites obtained from the Mössbauer data on the basis of the area of the fitted sextets is $(Zn_{0.5}Fe_{0.5})^A[Ni_{0.25}Co_{0.25}Fe_{1.5}O_4]^B$. Since there are four cations involved, the known relative strength of preference of occupation of sites[20] has been taken into consideration while calculating this distribution. In bulk Co-Zn ferrites, Zn is known to have strong preference for the A site while Co and Ni are known to have strong B-site preferences. Fitted parameters for core are given in Table I. Table II shows the fitted parameters for the shell and canting angles for shell is given in the Table III.

In bulk ferrites the sense of magnetization between the A and B sublattices is opposite so that these are antiferromagnetically coupled, leading to an overall ferrimagnetic ordering with net moments depending on the cation distribution. When a magnetic field large enough to saturate is applied, in the absence of spin canting, the hyperfine field at the A site will be parallel and that at the B site will be antiparallel to the applied field.[21] Therefore, the magnetic splitting of the A component is increased and the splitting of the B component is decreased, allowing a clear distinction between the A and

TABLE I. Mössbauer parameters for core for various measurements (field applied 5 T).

	Hyperfine field (T) ±0.03		Isomer shift (mm/s) ±0.05		Width (mm/s) ±0.05	
Type of measurement	*A*	*B*	*A*	*B*	*A*	*B*
ZFC (perpendicular)	54.9	46.1	0.27	0.308	0.452	0.55
FC (perpendicular)	54.22	46	0.276	0.326	0.452	0.55
ZFC (longitudinal)	53.99	47.25	0.271	0.356	0.55	0.65

TABLE II. Mössbauer parameters for shell for various measurements (field applied 5 T).

	Hyperfine field (T) ±0.03		Isomer shift (mm/s) ±0.05		Width (mm/s) ±0.05	
Type of measurement	*A*	*B*	*A*	*B*	*A*	*B*
ZFC (perpendicular)	52.9	49.0	0.25	0.28	0.51	0.62
FC (perpendicular)	51.8	48.5	0.29	0.32	0.45	0.72
ZFC (longitudinal)	51.5	48.9	0.29	0.37	0.55	0.89

TABLE III. Canting effects from shell for various measurements.

	θ (deg)[a]		H_{hf} (T)		ϕ (deg)[b]	
Type of measurement	*A*	*B*	*A*	*B*	*A*	*B*
ZFC (perpendicular)	54.7	54.7	50.2	52.0	59.4	50.2
FC (perpendicular)	54.7	54.7	48.8	51.6	59.5	50.2
ZFC (longitudinal)	58.7	59.9	49.1	51.6	63.7	55.2

[a]Angle between gamma-ray direction and the direction of total magnetic field.

[b]Angle between applied field and the magnetic hyperfine field.

B components. Moreover, the relative intensities of lines 2 and 5 in the sextets are affected by the direction of the applied field. When the field is applied parallel to the γ-ray direction, the intensities of the middle (2 and 5) peaks in a sextet become 0. It becomes 4 when the field is applied perpendicular to the γ rays. The intensity of peaks 1 and 3 (as also 6 and 4) is always 3:1. The magnetic splitting is determined by the total magnetic field B_T at the nucleus, which is given by the vector sum of the hyperfine field, B_{hf}, and the applied field, B_A. Thus, hyperfine field at the nucleus and the average canting angle can both be determined using the method described by Petitt and Forester.[21]

The experimental data for all three in-field Mössbauer spectra for nanosized $Ni_{0.25}Co_{0.25}Zn_{0.5}Fe_2O_4$ can be fitted satisfactorily with four sextets. Since the overall relative transmission is only about 6%, to obtain physically realistic values for individual line intensities, the relative intensity x of the middle peaks (lines 2 and 5 of a sextet) with respect to the inner peaks, $3:x:1:1:x:3$, has been constrained, as is necessary in many cases.[5] In all three spectra, two sets of sextets have a value of 2 for x, irrespective of the field direction. The other two sextets have a value of 4 for x when the field is applied perpendicular to the direction of γ rays and 0 when the field direction is parallel to γ rays. Comparing the relative intensities of the sextets and also the hyperfine fields, pairs of sextets in which the middle peak intensity is 0 or 4 also show a field shift exactly equal to double the applied field. The total difference between the two sextets is therefore equal to 8 T. The observed value of contraction/expansion is 4 T implying a demagnetizing field of 1 T.[22]

The other pair has x values equal to 2, indicative of random spin arrangement corresponding to an average angle of 54° with respect to the applied field direction. The hyperfine field values are nearly the same as that obtained with no applied field. Interestingly, there is no significant difference in the obtained parameters of the $ZFC_{perpendicular}$ and $FC_{perpendicular}$ cases. The sextets which show a collinear arrangements of spins, i.e, those with $x=0$ or 4 can thus be assigned to the core and the other pair with $x=2$ to Fe at the surface. These results, particularly the indistinguishibility of $FC_{perpendicular}$ and $ZFC_{perpendicular}$ show that the dominant contribution to the magnetization is from the shell and that the system can be compared to a model consisting of a well-ordered core and a surface layer of canted spins in which the applied field is sufficient to order the core while it has no effect on the shell. In this model, the thickness of the surface layer t can be calculated from the particle size d using the following relation:[8]

$$V_{canted} = 1 - \left(\frac{1-2t}{d}\right)^3, \tag{6}$$

where V_{canted} is the volume fraction of canted spins obtained from fit. Mössbauer studies show that almost 70% of Fe lies at the surface and the value of t obtained for the present system is 0.59 nm. Thus the core can be described by Neel's model in which the spins at the *A* and *B* sites are collinear but aligned in opposite directions whereas fields as large as 5 T do not affect the surface spins. On the basis of area ratios of individual set of sextets, the average cation distribution of the core and shell are the same showing that the chemical composition at the core and shell is the same.

IV. CONCLUSIONS

The measurements carried out in the present study very clearly establish that in the present sample, owing to the very small sizes, most of the spins are at the surface and so the magnetic properties are dominated by surface spins which are nearly impervious to fields on the order of 5 T as applied in the present studies. The system can be modeled as an ordered core with conventional collinear arrangement of spins at the *A* and *B* sites and a canted, highly frustrated surface. The effects observed are comparable to those obtained in nanoganular systems comprising of ferromagnetic particles embedded in an antiferromagnetic matrix. The large volume fraction of surface spins completely isolates the cores so that the entire ensemble behaves as a system of nearly perfectly noninteracting particles. dc magnetization studies also establish the fairly strong exchange bias which exists between the core and shell.

ACKNOWLEDGMENTS

We acknowledge financial support under the UGC-DSA and UGC-FIST schemes in the Department of Physics, Mohanlal Sukhadia University, Udaipur.

[1] Q. A. Pankhurst, J. Connolly, S. K. Jones, and J. Dobson, J. Phys. D **36**, R167 (2003).

[2] I. Safarik, M. Safaríková, and S. J. Forsythe, J. Appl. Bacteriol. **78**, 575 (1995).

[3] D. K. Kim, Y. Zhang, W. Voit, K. V. Rao, and M. Muhammed, J. Magn. Magn. Mater. **225**, 30 (2001).

[4] C. A. Ross, Annu. Rev. Mater. Res. **31**, 203 (2001).

[5] L. Theil Kuhn, A. Bojesen, L. Timmermann, M. Meedom

Nielsen, and S. Mørup, J. Phys.: Condens. Matter **14**, 13551 (2002).
[6] A. Labarta, X. Batlle, and O. Iglesias, *Surface Effects in Magnetic Nanoparticles* (Springer, New York, 2006), Chap. 4, pp. 105–140.
[7] L. Del Bianco, D. Fiorani, A. M. Testa, E. Bonetti, L. Savini, and S. Signoretti, Phys. Rev. B **66**, 174418 (2002).
[8] E. C. Sousa, M. H. Sousa, H. R. Rechenberg, G. F. Goya, F. A. Tourinho, R. Perzynski, and J. Depeyrot, J. Magn. Magn. Mater. **310**, e1020 (2007).
[9] A. Ceylan, S. K. Hasanain, and S. I. Shah, J. Phys. Condens. Matter **20**, 195208 (2008).
[10] O. P. Suwalka, R. K. Sharma, V. Sebastian, N. Lakshmi, and K. Venugopalan, J. Magn. Magn. Mater. **313**, 198 (2007).
[11] L. Wang and F. S. Li, J. Magn. Magn. Mater. **223**, 233 (2001).
[12] C. K. Ong, H. C. Fang, Z. Yang, and Y. Li, J. Magn. Magn. Mater. **213**, 413 (2000).
[13] W. H. Meiklejohn and C. P. Bean, Phys. Rev. **105**, 904 (1957).
[14] J. Nogués and I. K. Schuller, J. Magn. Magn. Mater. **192**, 203 (1999).
[15] A. E. Berkowitz and K. Takano, J. Magn. Magn. Mater. **200**, 552 (1999).
[16] J. Nogués, J. Sort, V. Langlais, V. Skumryev, S. Suriñach, J. S. Muñoz, and M. D. Baró, Phys. Rep. **422**, 65 (2005).
[17] L. Sun, P. C. Searson, and C. L. Chien, Phys. Rev. B **71**, 012417 (2005).
[18] J. García-Otero, M. Porto, and J. Rivas, J. Appl. Phys. **87**, 7376 (2000).
[19] L. Del Bianco, D. Fiorani, A. M. Testa, E. Bonetti, and L. Signorini, Phys. Rev. B **70**, 052401 (2004).
[20] R. K. Sharma, V. Sebastian, N. Lakshmi, K. Venugopalan, V. R. Reddy, and A. Gupta, Phys. Rev. B **75**, 144419 (2007).
[21] G. A. Petitt and D. W. Forester, Phys. Rev. B **4**, 3912 (1971).
[22] N. Blum and L. Grodzins, Phys. Rev. **136**, A133 (1964).